Measurement of the electrical properties of ungelled ECG electrodes

A. Baba and M. J. Burke

***Abstract*—**This paper reports the measurement of the properties of dry or pasteless conductive electrodes to be used for long-term recording of the human electrocardiogram (ECG). Knowledge of these properties is essential for the correct design of the input stage of associated recording amplifiers. Measurements were made on seven commercially available conductive carbon based electrodes at pressures of 5 mmHg (0.67 kPa) and 20 mmHg (2.7 kPa), located on the lower abdomen and chest of the body on seven subjects having different skin types. Parameter values were fitted to a two-time-constant based model of the electrode using data measured over a period of 10 s. Values of resistance, ranging from 23 kΩ to 1850 kΩ and of capacitance ranging from 0.01 μF to 65 μF were obtained for the components, while the values of the time-constants varied from 0.02 s to 7.2 s.

***Keywords*—** Electrodes, ECG Recording, ECG Amplifier.

I. Introduction

IN the long term recording of the human electrocardiogram (ECG) conventional jelled electrodes suffer from several disadvantages. Firstly, when applied to the body they are suitable for one-time-use only. Secondly, when used for more than a couple of days many patients develop allergic reactions or other forms of skin irritation. Finally, there is also the personal inconvenience of not being able to shower or bathe while using the electrodes. In recent years a small number of dry or pasteless conductive electrodes have been developed which overcome these disadvantages and interest in the use of these electrodes for long-term ambulatory ECG monitoring has increased [1], [2]. However, the performance requirements of the input stage of the associated recording amplifier are much more demanding in the case of dry electrodes than for conventional jelled electrodes. It has long been established that the skin-electrode interface introduces a phase shift into the received signal which can result in serious distortion of the ECG profile [3], [4]. Consequently, characterisation of the impedance of the skin-electrode interface provides essential information for the correct design of the amplifier for faithful reproduction of the ECG signal morphology.

A physical model which treats the skin-electrode interface as a double time constant system [5] is shown in Fig. 1. Because of complex current dependent voltage sources, capacitances, and resistors, the skin-electrode interface is, in reality, a time-varying non-linear system. The polarisation voltages are of no interest in this exercise and are not measured. Consequently, for the purposes of long term ECG monitoring, the six passive-element electrical equivalent model shown is adequate.

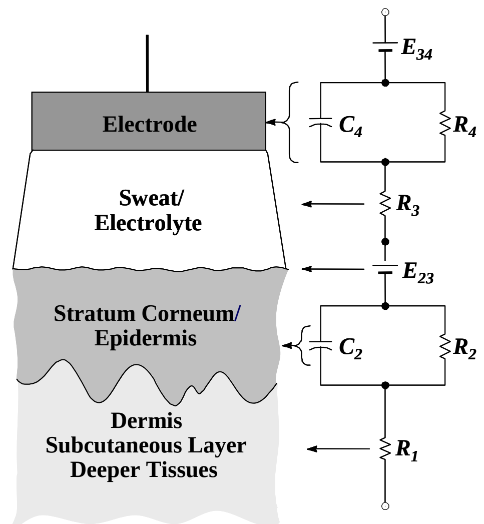

Fig. 1. Skin-electrode interface and its electrical equivalent circuit (modified from [3]).

II. Methodology

A. Current Source Measurement Circuit

The measurement method relies on the transient response of the skin-electrode interface to a rectangular current pulse having a long on-off mark-space ratio as well as a sine wave current. Fig. 2 illustrates the circuit diagram of a current source that feeds a constant current through the body while measuring the skin-electrode impedance. The current is switched on and off by a relay to provide an extremely high impedance when off. The relay opens and closes under the control of a square wave voltage source with a 60s period. The current can also be kept on and modulated by a sine wave source as shown in the figure.

The resistor divider R_5 and R_6 sets the potential, V_I^+, at the non-inverting input of the operational amplifier A_1. V_I^-, the potential at the inverting input of A_1 maintains a current, I_0, through the resistor, R_7, as:

$$I_0 = \frac{R_5 V_{cc}}{(R_5 + R_6) R_7} \tag{1}$$

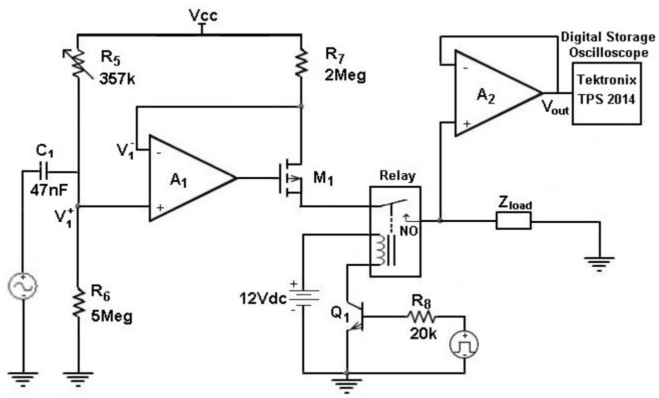

Fig. 2. Schematic Diagram of the current source circuit.

The P-channel MOS transistor, M_1, (3N163, Vishay Inc), allows a fixed output current to be supplied, independent of the load impedance. Finally, the operational amplifier, A_2, acts as a buffer which prevents the impedance of the measuring digital oscilloscope from shunting the impedance of the measured electrode. Op-amps (OPA602, Burr-Brown) having a very low offset voltage and bias current were used to minimise the effects of these on the measurements. In addition, a high frequency sine wave voltage is used to modulate the on value of current generated by the current source. This allows the sum of the series resistances $R_1 + R_3$ to be determined, as at relatively high frequencies the impedances of the capacitors C_2 and C_4 become extremely low and shunt the resistors R_2 and R_4.

B. Curve Fitting Procedure

Since the circuit has a limited rise and fall time of 0.5 ms, the response of the electrical equivalent circuit in Fig. 1 was determined, assuming an input current step to the system having an exponential rise and fall time constant $\tau_0 = 0.1$ ms. The resulting transient voltage measured at the output of the buffer amplifier, A_2, is given as:

$$v(t) = \left[(R_1 + R_3) + R_2 + R_4 - \frac{R_2 \tau_2}{\tau_2 - \tau_0} e^{-t/\tau_2} - \frac{R_4 \tau_4}{\tau_4 - \tau_0} e^{-t/\tau_4} + \left[\frac{R_2 \tau_0}{\tau_2 - \tau_0} + \frac{R_4 \tau_0}{\tau_4 - \tau_0} - (R_1 + R_3) \right] e^{-t/\tau_0} \right] I_0 \tag{2}$$

where $\tau_2 = C_2R_2$, $\tau_4 = C_4R_4$ and I_0 is the injected current set at 1μA.

A least-mean-square error minimization program was developed in MatLab (MathWorks Inc.), in order to extract the parameters of the skin-electrode model from the measured data. The rise and fall phases of the response shown in Fig. 3 are fitted independently, using the following equations:

$$v_{rise}(t) = V_{inR} + 2v(t) \tag{3}$$

$$v_{fall}(t) = V_{inF} - 2v(t) \tag{4}$$

where V_{inR} and V_{inF} are the initial values of the output voltage for the rise and fall phases, respectively and are taken as the values present immediately preceding a rise or fall phase just before the switching of the relay.

The values of series resistance, $R_1 + R_3$, determined using the high frequency sinusoidal current are input directly into the algorithm, reducing the complexity of the fitting procedure to only four parameters.

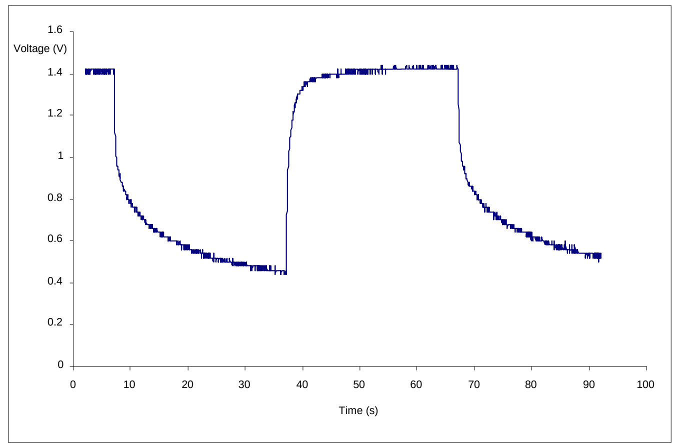

Fig. 3. Illustration of the rise and fall phases of the voltage response.

C. The Measurement Procedure

Measurements were performed on seven subjects, using seven types of commercially available dry electrodes at normal room temperature. The skin was not prepared in any form but the electrodes were disinfected with an alcohol wipe before each measurement. Two locations were considered on each subject, the lower abdomen, a relatively hair-free area and the chest. For each location and electrode type, measurements were carried out at two pressure levels of 5 mmHg (0.67 kPa) and 20 mmHg (2.7 kPa). The electrodes were placed about 10 cm apart at each location. A purpose built adjustable belt was used to hold the electrodes in place. The belt is fitted with a bladder which can be inflated to apply the required pressure level. The electrodes were left in place for 20 minutes during which time the subject sat comfortably on a chair to allow time for stabilisation of the conductive layer formed by natural perspiration of the skin, so that values measured would be representative of those which exist in a long-term ECG recording scenario. The pressure was measured and monitored with a precision pressure monitor (model RPM3, DH Instruments Inc.,). At the end of the stabilisation time, subjects were asked to sit still so that excessive muscular movement would not distort the exponential voltage waveform to be measured. The circuit board and the measurement set-up were designed to permit a quick change over from the time based measurement mode to the amplitude modulation based measurement. This helped to reduce the time required for each measurement.

D. The Electrodes

Seven different types of flexible, dry, body-surface, carbon-inlayed silicone rubber electrodes were subjected to measurement in this study. The electrodes are commercially available and were sourced from Wandy Rubber Industrial Co. and Canadian Medical Products Ltd (CanMed).

Wandy Rubber Industrial Co.

1) WA-45: circular, active area 10.75 cm^2, rough surface;

2) WA-65: circular, active area 25.50 cm^2, rough surface;

3) WA-QO4: rectangular, active area 45 cm^2, smooth surface;

Canadian Medical Products Ltd.

4) Pro Carbon C5005PF: circular, active area 4.9 cm^2, smooth surface;

5) Pro Carbon C5120PF: circular, active area 11.3 cm^2, smooth surface;

6) Pro Carbon C5010PF: rectangular, active area 17.1cm^2, smooth surface.

7) Pro Carbon C5020PF: rectangular, active area 45 cm^2, smooth surface.

E. The Subjects

Relevant details of the seven subjects who participated in the study are summarised in Table I.

Table I Details of subjects.

Subject	Skin Type	Sex	Age (years)
1	White	Male	59
2	White	Male	24
3	Black	Male	24
4	Black	Male	28
5	White	Female	26
6	White	Female	25
7	Black	Female	22

III. RESULTS

A. Validation of Fitting Procedure

In order to determine the accuracy and the error associated with the curve fitted to the measured data using the fitting algorithm, a simulation of the model was performed using PSpice. The resulting voltage data were used in the curve fitting algorithm to extract the parameters of the circuit used in the PSpice model. The results of the curve fitting compared to the values of the components in the simulated circuit are presented in Table II.

A maximum percentage error of 5.6 % was observed in the values of resistance and capacitance obtained from the curve fitting compared to the actual simulation values.

Table II Fitting results for the simulated circuit.

	Simulated values	Fitting results rise phase	Fitting results fall phase
R_1+R_3(kΩ)	10.0	10.0	10.0
R_2 (kΩ)	440.0	446.2 (+1.4%)	446.7 (+1.5%)
C_2 (μF)	0.50	0.51 (+2.0%)	0.51 (+2.0%)
τ_2 (s)	0.220	0.229 (+4.1%)	0.227 (+3.2%)
R_4 (kΩ)	220.0	214.0 (-2.7%)	213.2 (-3.1%)
C_4 (μF)	6.60	6.91 (+4.7%)	6.97 (+5.6%)
τ_4 (s)	1.452	1.479 (+1.9%)	1.486 (+2.3%)

Following the PSpice circuit simulation, a hardware circuit similar to the skin-electrode interface equivalent model was constructed on a breadboard. Component values were selected similar to the ones used in the PSpice simulation and the circuit was driven with the same current source designed for use in the in vivo measurements. The recorded voltage data were then entered into the curve fitting algorithm and the resulting parameter values obtained were compared with the hardware components. The parameters determined through the fitting procedure applied to the rise and fall phases of the response are listed in Table III. In this measurement, the percentage errors are higher with respect to those shown in Table II, due to the tolerance in the values of the components and the quantization error of the measuring oscilloscope.

Table III Fitting results for the constructed circuit.

	Circuit values	Fitting results rise phase	Fitting results fall phase
R_1+R_3(kΩ)	10.2	10.2	10.2
R_2 (kΩ)	439.0	437.0 (-0.5%)	428.8 (-2.3%)
C_2 (μF)	0.51	0.56 (+9.8%)	0.58 (+13.7%)
τ_2 (s)	0.224	0.245 (+9.4%)	0.248 (+10.7%)
R_4 (kΩ)	220.9	208.6 (-5.6%)	217.0 (-1.8%)
C_4 (μF)	6.65	7.08 (+6.5%)	6.78 (+2.0%)
τ_4 (s)	1.469	1.476 (+0.5%)	1.472 (+0.2%)

B. Results for Skin-Electrode Measurement

The in-vivo measurements comprised of 28 separate measurements on each subject. That is, seven electrodes were subjected to measurements, located on either the chest or lower abdomen, with applied electrode application pressure of 5 mmHg or 20 mmHg in each case. Table IV presents one set of results obtained, using the Wandy WA-45 electrode on all subjects with the electrodes located on the abdomen at each of the two pressure levels. A summary of the component values obtained across all subjects, electrode types, locations and electrode application pressures is presented in Table V. These

Table IV Measurement results on the seven subjects using the WA-45 electrode located on the abdomen.

Parameters			Electrode location: abdomen				Electrode type: Wandy WA-45			Electrode contact pressure
			R_{13} (kΩ)	R_2 (kΩ)	C_2 (μF)	τ_2 (s)	R_4 (kΩ)	C_4(μF)	τ_4 (s)	
			Parameter values for voltage rise phase							20mmHg (2.7kPa)
Subject & skin type	1	White	2	580	0.17	0.1	580	1.72	1	
	2	White	1.28	203.44	0.91	0.19	171.2	9.34	1.6	
	3	Black	6	1,274.29	0.06	0.08	852.85	0.44	0.38	
	4	Black	1.7	1,094.76	0.11	0.12	177.21	8.6	1.52	
	5	White	1.28	222.32	0.87	0.19	212.61	10.52	2.24	
	6	White	1.28	60.52	2.48	0.15	178.66	12.24	2.19	
	7	Black	1.97	592.9	0.3	0.18	331.37	4.14	1.37	
			Parameter values for voltage fall phase							
Subject & skin type	1	White	2	244.21	0.63	0.15	225.93	15.15	3.42	
	2	White	1.28	100.55	1.36	0.14	176	28.64	5.04	
	3	Black	6	1,671.04	0.12	0.2	378.35	6.42	2.43	
	4	Black	1.7	941.54	0.14	0.13	388.7	6.45	2.51	
	5	White	1.28	191.91	0.89	0.17	188.06	19.91	3.74	
	6	White	1.28	66.22	2.6	0.17	142.9	31.97	4.57	
	7	Black	1.97	567.48	0.34	0.19	257.4	10.17	2.62	
			Parameter values for voltage rise phase							5mmHg (0.67kPa)
Subject & skin type	1	White	2.48	391.57	0.45	0.18	168.62	8.41	1.42	
	2	White	1.84	359.72	0.48	0.17	235.84	6.72	1.58	
	3	Black	3.92	781.53	0.17	0.13	185.94	5.76	1.07	
	4	Black	1.6	975.69	0.1	0.1	246.31	3.42	0.84	
	5	White	1.52	223.97	0.68	0.15	245.11	5.45	1.34	
	6	White	6.32	1,462.30	0.04	0.06	819.22	0.5	0.41	
	7	Black	2.08	625.49	0.32	0.2	349.59	4.37	1.53	
			Parameter values for voltage fall phase							
Subject & skin type	1	White	2.48	296.45	0.48	0.14	199.34	19.85	3.96	
	2	White	1.84	310.77	0.52	0.16	214.29	16.76	3.59	
	3	Black	3.92	560.26	0.36	0.2	276.4	13.52	3.74	
	4	Black	1.6	909.48	0.12	0.11	334.49	6.75	2.26	
	5	White	1.52	210.23	0.67	0.14	210.33	19.94	4.19	
	6	White	6.32	1,535.18	0.08	0.12	549.8	3.76	2.07	
	7	Black	2.08	598.67	0.36	0.22	271.55	10.73	2.91	

Table V Summary of values for each component, measured across all subjects, electrodes, locations and pressures.

	R_{13}(KΩ)	R_2(KΩ)	C_2(μF)	τ_2 (s)	R_4(KΩ)	C_4(μF)	τ_4 (s)	R_{1234}(KΩ)
Voltage rise phase								
minimum	0.64	4.94	0.01	0.02	23.26	0.1	0.18	161.24
maximium	12	1,760.24	21.51	1.84	1,850.52	432.35	31.29	3,616.83
Voltage fall phase								
minimum	0.64	23.87	0.04	0.06	84.78	0.69	0.77	125.82
maximum	12	2,540.93	21.88	1.17	1,380.00	65.15	7.19	3,326.10

Table VI Measurement results for varying current level on subject 4.

WANDY WA- 45 subject 4

current level(μA)	R_{13} (kΩ)	R_2 (kΩ)	C_2 (μF)	τ_2 (s)	R_4(kΩ)	C_4 (μF)	τ_4 (s)
Parameter values for voltage rise phase							
0.5	1.02	1,253.30	0.36	0.45	377.21	10.24	3.86
1	1.7	1,094.76	0.11	0.12	177.21	8.6	1.52
2	3.52	430.61	0.33	0.14	119.51	17.41	2.08
5	5.76	306	0.28	0.09	109	2.81	0.31
10	17.4	228.18	0.37	0.08	31.67	33.54	1.06
20	7.6	84.08	1.41	0.12	20.01	26.42	0.53
Parameter values for voltage fall phase							
0.5	1.02	1,154.70	0.35	0.41	416.67	17.69	7.37
1	1.7	941.54	0.14	0.13	388.7	6.46	2.51
2	3.52	409.13	0.2	0.08	99.57	12.46	1.24
5	5.76	299.57	0.31	0.09	97.46	18.56	1.81
10	17.4	195.92	0.5	0.1	48.84	27.94	1.36
20	7.6	108	0.93	0.1	108	9.26	1

CanMed C5120PF

current level(μA)	R_{13} (kΩ)	R_2 (kΩ)	C_2 (μF)	τ_2 (s)	R_4(kΩ)	C_4 (μF)	τ_4 (s)
Parameter values for voltage rise phase							
0.5	0.98	841.25	0.31	0.26	190.64	15.26	2.91
1	1.7	472.35	0.28	0.13	47.66	30.41	1.45
2	3.02	421.36	0.33	0.14	116.94	17.04	1.99
5	5.64	401.35	0.27	0.11	68.35	26.46	1.81
10	15.64	223.27	0.36	0.08	30.99	32.82	1.02
20	19.26	82.28	1.38	0.11	19.58	25.86	0.51
Parameter values for voltage fall phase							
0.5	0.98	799.89	0.36	0.29	484.56	17.69	0.37
1	1.7	451.67	0.33	0.15	121.14	17.48	2.12
2	3.02	409.04	0.19	0.08	99.04	1.92	0.19
5	5.64	317.03	0.3	0.1	74.26	21.46	1.59
10	15.64	191.71	0.49	0.09	47.79	27.33	1.31
20	19.26	105.68	0.91	0.1	105.68	9.06	0.96

are the minimum and maximum values obtained for each individual parameter across all the measurements.

C. Results for Current Levels other than 1μA

In order to establish the effect of the current level used on the measured impedance, additional measurements were performed on Subjects 4 and 5 using current levels of 0.5, 2, 5, 10 and 20 μA. The measurement procedure in each case is the same as for 1 μA, but only the Wandy WA- 45 and CanMed C5120PF electrodes were used in this case. The results on Subject 4 showing the variation in the component value at each current level are presented in Table VI.

D. Results for Different Electrode Settling Times

Dry electrodes seldom remain dry after prolonged application due to sweat build up on the skin. The accumulation of sweat also tends to lower the interface impedance due to improved conductivity. Additional measurements were performed on Subjects 4 and 5 immediately upon the attachment of the electrodes and at regular time intervals over a 40 minute period. The results showing an initial rapid reduction and then steady state component values after sufficient time has elapsed are shown in Table VII for Subject 4.

IV. Discussion

The parameter values obtained from the measurements as presented in Tables IV and V show a wide spread. Values vary considerably for the resistive and capacitive components but there is less variation between time constants for corresponding measurement conditions. It can be seen that there are two definite time constants present which are typically an order of magnitude apart for a given electrode, subject and applied pressure. However, in some cases the separation is significantly greater or less than this. In addition, corresponding time constants vary by as much as a factor of 2:1 between subjects for the same measurement conditions. The same can be said regarding time constant variation with applied pressure. It is clear that there are substantial differences in the component values and the time constants measured during rise and fall phases of the response. Attempts to fit the same set of time constants to both rise and fall phases failed definitively. Variation in component values were also observed in measurements performed at the hairy and non-hairy locations, with the hairy location resulting in higher interface impedance. Comparison of results between genders reveals that the female subjects exhibit higher impedance compared with the male subjects for similar skin type. Measurements performed at the lower electrode application pressure resulted in higher contact impedance. Small-sized electrodes resulted in higher skin-electrode interface impedance. Increased current level caused a reduction in the measured impedance. Attempts to perform the measurement at a current level below 1 μA failed because of the low signal to noise ratio. The overall interface impedance tends to reduce with prolonged electrode settling time. This is more rapid in the first few minutes after application and the values tend to stabilise after about 20 minutes. This can be seen in the plots of Fig. 4.

V. Conclusion

Based on the parameters extracted, the dc resistance, $R_1+R_2+R_3+R_4$, of the skin-electrode interface have been established to range between 125 kΩ and 3.6 MΩ for different electrode sizes, skin types, gender, body locations and electrode application pressures. The measurement results have been used as the basis for the design of the front-end amplifier of an ECG recording system using dry electrodes. The performance requirements recommended by the American Heart Association (AHA) and the European Union (EU601) for ECG recording systems states that, the phase shift introduced by the ECG recording system should be no more than that introduced by an analogue 0.05 Hz single-pole high-pass filter, if the T-wave and ST segment of the ECG profile are to be preserved [6], [7]. Furthermore, to prevent the attenuation of the measured ECG signal, the input impedance of the front-end amplifier must be much higher than that of the skin electrode interface. It can be shown that the minimum differential amplifier input impedance, R_d, required to satisfy the AHA and EU601 phase requirements is given by:

$$R_d > \frac{1}{2\pi * 0.05} * 2\left(\frac{R_2}{\tau_4} + \frac{R_4}{\tau_2} + \frac{1}{C_{in}}\right) \tag{5}$$

where R_2, R_4, τ_2, τ_4 are the equivalent circuit model parameters as have been measured and C_{in}, is the value of the capacitor used to ac couple the ECG signal to the amplifier input in order to block dc potentials [8].

If C_{in} is taken as 0.33 μF, the maximum component values measured for the electrodes examined on each subject can be used to determine the minimum requirement for the input resistance of the amplifier as 590 MΩ. The input resistance referred to here is, in effect, the differential and common mode input resistances of the amplifier seen in parallel. It should be noted that the highest values result universally from the smallest sized electrodes. This is particularly true for the results on Subject 6. The smallest sized electrodes on this subject resulted in an amplifier input impedance requirement value of 590 MΩ and 249 MΩ for measurements taken at 5 mmHg and 20 mmHg respectively, while the maximum requirement across all other electrode types on this subject is 130 MΩ.

This value can be validated in a simulation by superimposing the phase response of the circuit model with the recommended resistive amplifier input impedance, on that of an analogue 0.05 Hz single-pole high-pass filter. The resulting family of phase response curves is shown in Fig 4. It can be observed that for a resistive amplifier impedance of 130 MΩ, the phase shift introduced by the electrode model for Subject 6 is slightly outside of the specification. However, the absolute value of this phase difference is less than 0.25 degrees which is negligible and it cannot be ascertained that this will introduce any appreciable distortion in the measured ECG that will affect its diagnostic quality. In conclusion, it is recommended that the input impedance of the recording amplifier should be at

Table VII Measurement result for varying electrode settling time on subject 4.

WANDY WA-45 subject 4

Time (minute)	R_{13} (kΩ)	R_2 (kΩ)	C_2 (μF)	τ_2 (s)	R_4 (kΩ)	C_4 (μF)	τ_4 (s)
			Rise phase				
1	6.42	2,884.96	0.01	0.03	462.41	0.99	0.46
5	4.84	1,813.66	0.05	0.1	419.65	4.76	2
10	3.74	1,479.36	0.07	0.11	325.1	4.96	1.61
15	2.56	1,198.49	0.09	0.11	279.8	5.35	1.5
20	1.7	1,094.76	0.11	0.12	277.21	8.9	2.47
25	1.64	908.15	0.37	0.34	254.36	10.16	2.58
30	1.62	877.5	0.5	0.43	243.2	14.35	3.48
40	1.56	860.92	0.56	0.48	240.4	17.46	4.19
			Fall phase				
1	6.42	2,713.03	0.06	0.15	416.66	4.44	1.85
5	4.84	1,705.57	0.25	0.42	388.47	9.74	3.78
10	3.74	1,391.20	0.32	0.44	305.59	11.57	3.54
15	2.56	1,127.07	0.45	0.51	263.01	13.73	3.61
20	1.7	1,029.51	0.14	0.15	260.57	15.46	4.03
25	1.64	854.03	0.61	0.52	239.1	19.21	4.59
30	1.62	825.21	0.71	0.58	228.61	22.17	5.07
40	1.56	809.62	0.59	0.48	225.97	24.04	5.43

CanMed C5120PF

			Rise phase				
1	6.42	1,964.52	0.04	0.07	301.73	3.75	1.13
5	4.84	1,023.74	0.09	0.09	297.1	3.38	1
10	3.74	835.96	0.12	0.1	270.44	4.72	1.28
15	2.56	661.91	0.22	0.15	255.73	11.15	2.85
20	1.7	492.35	0.28	0.14	247.66	18.41	4.56
25	1.64	460.03	0.56	0.26	210.57	19.13	4.03
30	1.62	447.67	0.74	0.33	228.8	17.01	3.89
40	1.56	400.03	0.72	0.29	207.38	13.28	2.75
			Fall phase				
1	6.42	1,885.94	0.09	0.18	297.8	4.88	1.45
5	4.84	982.79	0.22	0.22	293.24	9.44	2.77
10	3.74	802.52	0.24	0.19	266.92	10.16	2.71
15	2.56	635.43	0.48	0.3	252.4	13.75	3.47
20	1.7	472.66	0.33	0.15	244.44	17.48	4.27
25	1.64	441.63	0.59	0.26	207.83	19.25	4
30	1.62	429.76	0.65	0.28	225.83	22.26	5.03

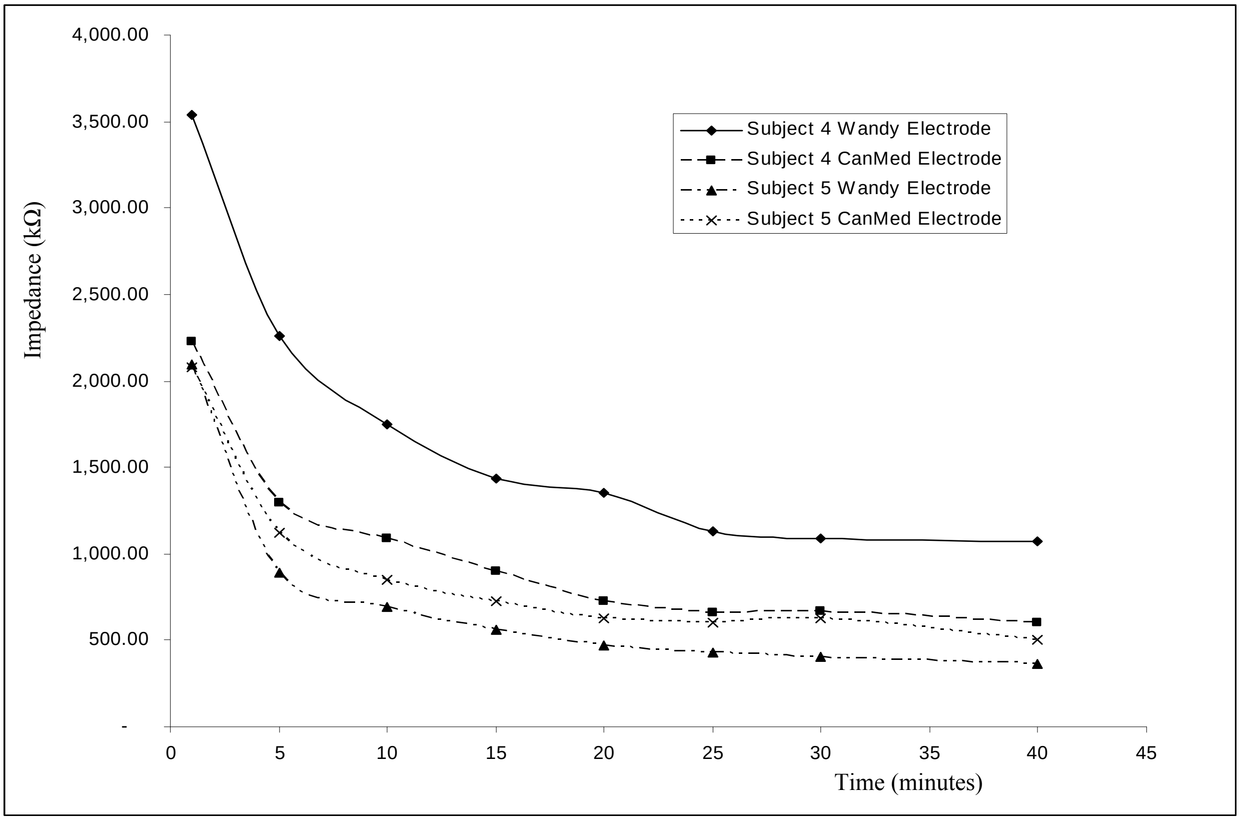

Fig. 4. Variation of impedance with electrode settling time on subjects 4 and 5.

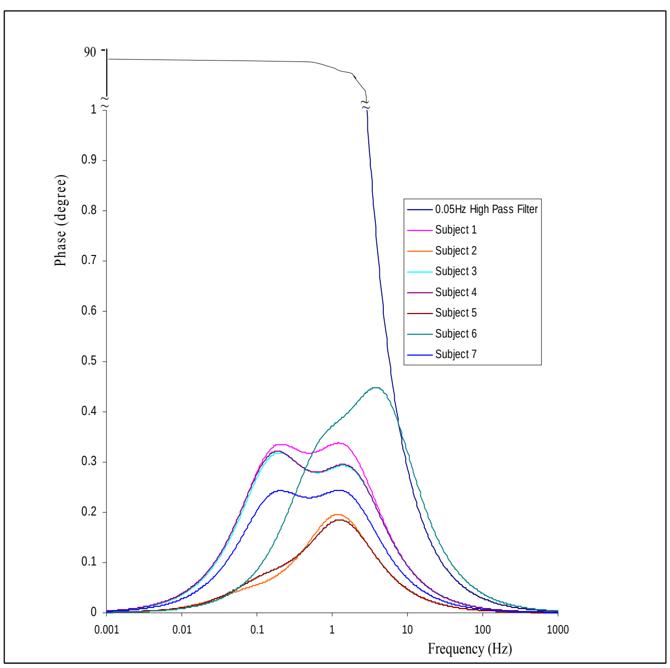

Fig. 5. Comparison of the phase response of the circuit model using values measured on different subjects with an amplifier input impedance of 130 MΩ and the phase response of a 0.05 Hz single-pole high-pass filter.

least 300 MΩ. This value of amplifier input impedance reduces the phase error for the smallest electrode on Subject 6 to less than 0.1 degrees.

References

[1] J. Muhlsteff and O. Such, "Dry electrodes for monitoring of vital signs in functional textiles," in *Proc. 26th Ann. IEEE Int. Conf. Eng. Med. & Biol. Soc.*, San Francisco, 2004, pp. 2212–2215.

[2] Puurtinen, M.M., *et al* "Measurement of noise and impedance of dry and wet textile electrodes, and textile electrodes with hydrogel". in *Proc. 28th Ann. IEEE Int.. Conf. Eng. Med. & Biol. Soc.*, San Francisco, 2006, pp. 6012-6015.

[3] S. Berson and H. V. Pipberger, "The low frequency response of electrocardiographs: a frequent source of recording errors," *Amer. Heart J.*, vol. 71, no. 6, pp. 779-789, July 1966.

[4] D. Tayler and R. Vincent, "Signal distortion in the electrocardiogram due to inadequate phase response," *IEEE Trans. Biomed. Eng.*, vol. 30, no. 6, pp. 352-356, June 1983.

[5] M. R. Neuman, "Biopotential Electrodes," in *Medical Instrumentation Application and Design*, 3rd ed., J. G. Webster, Ed. New York: John Wiley and Sons, 1998, pp. 183–232.

[6] J. J. Bailey *et al*, "AHA Scientific Council Special Report: Recommendations for standardization and specifications in automated electrocardiography", *Circulation*, vol. 81, no. 2, pp. 730–739, February 1990.

[7] European Commission, Directive IEC 601-1 / EN 60601-2-27, 1996, 'Medical Electrical Equipment – Part 2-27: Particular Requirements for the Safety of Electrocardiographic Monitoring Equipment'.

[8] C. Assambo, A. Baba, R. Dozio and M. J. Burke, "Parameter Estimation of the Skin-Electrode Interface Model for High-Impedance Bio-Electrodes"; *WSEAS Trans. Biol. & Med.*, vol. 3, issue 8, pp. 573-580, August 2006.